Caspian Journal of Environmental Sciences
Online ISSN: 1735-3866
Print ISSN: 1735-3033

Spatial evaluation of methane emissions in the communities of Warints and Yawi, Ecuador

Sandra- López[1]*, Juan- Haro[1], Carla – Haro[1], William- Carrillo[1], Justo Moises Narvaez Brito[2], Burkhanov Aktam Usmanovich[3], Ulugbek Tulakov[4], Tulovov Erkinjon[5], Mullabayev Baxtiyarjon[6], Mansurov Zuxriddin Xalilillayevich[7]

1. Escuela Superior Politècnica de Chimborazo (ESPOCH), Macas, Ecuador
2. Independent Researcher, Macas, Ecuador
3. DSc in Economics, Professor, International School of Finance and Technology, Tashkent, Uzbekistan & Alfraganus University, Tashkent, Uzbekistan
4. Termez State University, Termez, Uzbekistan
5. Tashkent State University of Economics, Tashkent, Uzbekistan
6. Namangan Engineering-Construction Institute, Namangan, Uzbekistan
7. Tashkent National Research University Institute of Irrigation and Agricultural Mechanization Engineers, Tashkent Uzbekistan, & Senior lecturer of the Tashkent University of Architecture and Civil Engineering, Tashkent, Uzbekistan, & Western Caspian University, Scientific researcher, Baku, Azerbaijan

** Corresponding author's Email: salopez@espoch.edu.ec*

ABSTRACT

Methane is a greenhouse gas that has caused environmental repercussions on the planet. At the national level, spatial data are unavailable, so this study aimed to estimate the amount of methane (CH_4) emissions in the communities of Warints and Yawi through satellite images. The methodological process was non-experimental, with a descriptive–longitudinal design; 3 satellite images were taken from the OLI and TIRS 8 sensor from the virtual repository (USGS Earth Explorer), years 2013, 2016, and 2020; ArcGIS and ENVI were used during preprocessing and processing: Normalized Difference Vegetation Index (NDVI), emissivity, surface temperature, and methane emissions were determined through the empirical model based on temperatures. The results were the following: for 2013, 2016, and 2020, it was 1.74×10^{-5}; 1.01×10^{-4}, and 2.36×10^{-4} megatons, respectively, with an annual emission rate of 45.11%. It is concluded that emissions are inversely proportional regarding community centers and bare soils. This model is recommended for estimating the annual methane budget in areas with high vegetative incidence at the local and regional levels.

Keywords: Methane, Remote sensing, Landsat, NDVI, Surface temperature, Sustainable development, Environmental economics.
Article type: Research Article.

INTRODUCTION

Currently, greenhouse gases along with global warming are receiving importance, due to the environmental repercussions they have generated on the planet (El-Hattab *et al.* 2018) . Methane plays a vital role in these processes, maintaining a relative potential 80 times greater than carbon (CO_2) to trap heat in the atmosphere over a period of 20 years (Arteaga 2017) . Although the emission sources are both natural and anthropogenic, their values have increased due to human activity by 60% of total emissions (Sun *et al.* 2017). The main sources are agriculture and livestock, the extractive industry (production of natural gas, oil, burning of biomass and coal; Puliafito *et al.* 2020) . These activities generate emissions both during normal operations and problems during operation (Sanucci 2021). There are several ways to estimate the amount of methane in the atmosphere, one of them is remote sensing, where satellites are used to observe the flow of gases in a certain area (Akumu *et al.*

Caspian Journal of Environmental Sciences, Vol. 23 No. 1 pp. 71-80 Received: April 22, 2024 Revised: July 13, 2024 Accepted: Sep. 27, 2024
DOI: 10.22124/CJES.2025.8366

Publisher: University of Guilan,

2010). Remote sensing provides products related to environmental variables necessary for estimation such as surface temperature (TS) and Normalized Difference Vegetation Index (NDVI). The first study regarding the use of satellite images was by Agarwal & Garg (2009) , where they presented an empirical model with MODIS data based on surface temperature to estimate methane (CH_4) in wetlands of Australia. This is where the importance of establishing a model based on temperatures arises. Likewise, Akumu *et al.* (2010) applied this model with Landsat ETM+ images in Australia considering the different environmental conditions that the place presented.
In Ecuador there are very few methane estimation studies with satellite images; they have been based more on the field of solid waste, such as the case of Ambuludi *et al.* (2022) in Pelileo, Tungurahua, through using LandGEM model, an equation based on the waste decomposition rate. Noting that the Emissions Database for Global Atmospheric Research (EDGAR) of Ecuador only provides generalized and non-spatial numerical data at the national level, this study is created with the objective of estimating the amount of methane (CH_4) emissions in the communities of Warints and Yawi through satellite images with the empirical model based on surface temperature (TS) and Normalized Difference Vegetation Index (NDVI), for the periods 2013, 2016 and 2020. as well as generating maps that help in decision-making and good judgment, as well as to mitigate this phenomenon, contributing to the communities in the sector.

MATERIALS AND METHODS

The research used a non-experimental methodology, with a descriptive – longitudinal design. It is divided into the following stages: Definition of the study area, preprocessing (image corrections) and data processing, within the processing variables are determined through calculations such as: NDVI, vegetation proportion, emissivity, brightness temperature, temperature surface, temperature factor and methane emission values. The methodological process is summarized in the following diagram (Fig. 1).

Study area

The communities of Warints and Yawi are in the Limón Indanza canton in the parish of San Antonio, bordering to the north with the Santiago de Méndez canton; to the south with San Juan Bosco; to the east with Peru and to the west with the province of Azuay. These communes are separated by a distance of approximately 1.9 km and 120 km from the capital city of Macas. They are located at the geographical coordinates 3° 4' 23.98" S and 78° 20' 19.35" W. The altitude is between 1,200 and 1,600 m above sea level. The climate is temperate and humid, the average temperature is between 18 °C and 22 ºC. The amount of precipitation is between 1500 mm and 3000 mm (PDOT 2015) . In this study, an area of 107.62 km^2 was taken as an area of analysis, since these are two communities that are not yet restricted in national registries.

Data source and preprocessing

Earth Explorer website of the Landsat 8 satellite, OLI and TIRS 8 sensors, extracting data from 11 spectral bands such as thermals, with a cloudiness of 30% and a resolution of 30 × 30 m pixelation; A Universal Transverse Mercator (UTM) projection was considered, zone 17 S with trajectory: 009, line: 069 of the following dates: September 2, 2013, January 14, 2016 and August 4, 2020 (due to the large number of clouds that the Ecuadorian Amazon presents was extracted only for three dates). Before starting the data analysis, preprocessing was applied, thus eliminating the interruptions that the data presented in terms of aerosol and radiance effects (Janampa & Ponce 2022) . Consequently, radiometric and atmospheric corrections were established through the ENVI 5.3 application, using the Radiometric tools. Calibration and Flash, consecutively. A cut was made due to the extension of the image with its extension Subset Data from ROIs. Finally, to have a clearer idea about its vegetation, a combination of bands was applied (Fig. 3), this being the most optimal to perceive healthy vegetation and grasslands (Suárez & Acosta 2020).

Processing of satellite images

The methodology of the present study was based on the study by Akumu *et al.* (2010) , thus establishing an empirical model that allowed methane emissions to be estimated depending on the surface temperature of the area (Cortez 2015).

Normalized Difference Vegetation Index (NDVI)

To calculate the empirical emission model, preprocessing is taken into account, to also determine the NDVI, whose values are determined through bands 5 and 4 (near infrared band and red band, respectively). The NDVI is

the phytosanitary indicator that allows distinguishing areas with vegetation from other areas possessing vegetation as well as distinguishing healthy vegetation from aged or stressed vegetation (Bautista *et al.* 2019) . NDVI values range from -1 to 1, with higher values indicating more vegetation present and lower values indicating less vegetation present (Sucapuca Mamani 2021). Calculating NDVI is vitally important for calculating the proportion of vegetation (V) and is closely related to emissivity (ε). Equation 1 (Avdan & Jovanovska 2016) was used for its calculation.

$$NDVI = \frac{NIR(Banda\ 5) - R(Banda\ 4)}{NIR(Banda\ 5) + R(Banda\ 4)} \quad \textbf{(1)}$$

where NIR represents the near-infrared band of Band 5 and R represents the red band of Band 4.

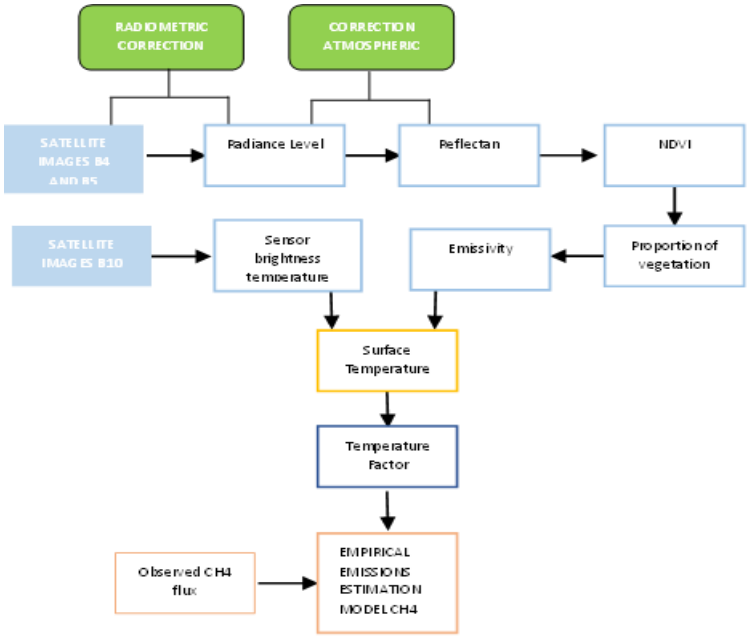

Fig. 1. Sequential process for estimating methane (CH_4) emissions in the Warints and Yawi communities through satellite images.

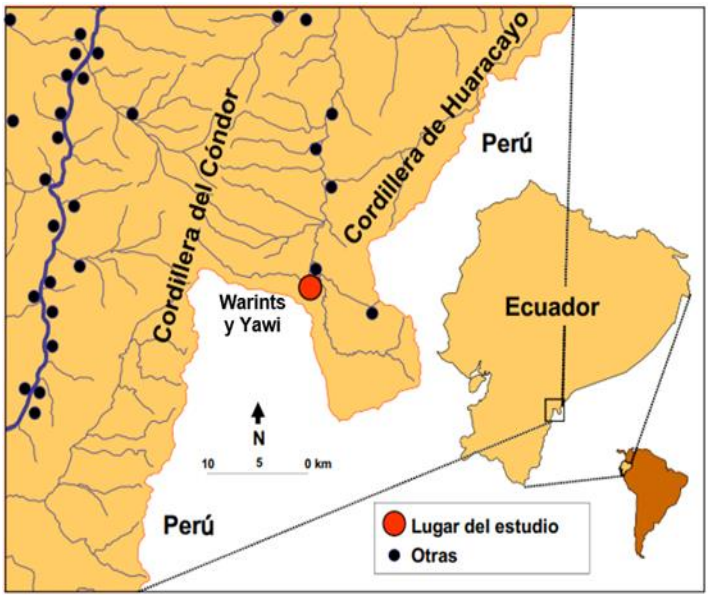

Fig. 2. Location map of the Warints and Yawi communities, Limón Indanza.

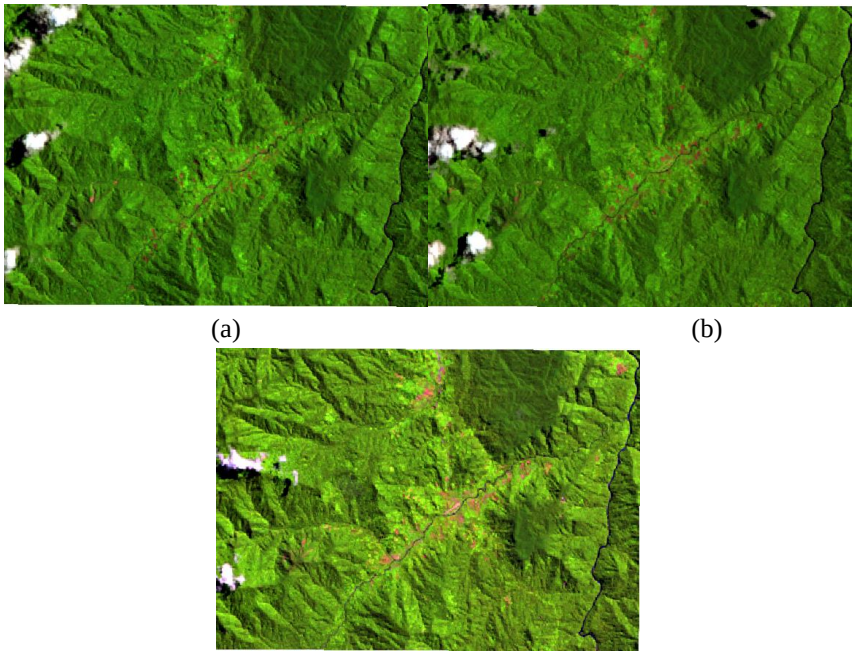

(a) (b)

(c)

Fig. 3. Combination of bands 6-5-2 of the OLI and TIRS 8 sensor from the Warints and Yawi communities; (a) September 2, 2013; (b) January 14, 2016; and (c) August 4, 2020.

Vegetation proportion (Pv)

This variable will be necessary to determine the emissivity values, being established from the NDVI values. Using the ArcGIS software, the maximum and minimum values of its pixels were determined. Equation 2 provided by Avdan & Jovanovska (2016) was used.

$$P_v = \left(\frac{NDVI - NDVI_{min}}{NDVI_{max} - NDVI_{min}}\right)^2 \quad \textbf{(2)}$$

where $NDVI_{min}$ and $NDVI_{max}$ are the minimum and maximum values of the NDVI map generated above.

Surface emissivity (ελ)

Emissivity was calculated from vegetation potential values and used to determine surface temperature. Emissivity is defined as the ratio between the energy emitted by a surface at a given wavelength as well as temperature and the energy emitted by a black body at the same wavelength and temperature (Sucapuca Mamani 2021). The emissivity was calculated using the formula provided by Stathopoulou *et al.* (2007) , where vegetation values are used. This proportionality variable is based on Planck's law where it scales the blackbody glow to predict its emitted value and its atmospheric thermal efficiency (Sucapuca Mamani 2021). The characteristics of the satellite images were adapted to the emissivity through formulations with simplified Equation 3 (Hantson *et al.* 2011).

$$\varepsilon\lambda = 0.004 \times P_v + 0.986 \quad \textbf{(3)}$$

where 0.004 is the emissivity constant of the vegetation and soil, while 0.986 is the surface roughness.

Radiance at brightness temperature (TB)

The ArcGIS software was used for its calculation through the Raster calculator. Equation 5 established in the study by Coelho & Correa (2013) was applied, thus using band 10 as radiance values; thermal calibration constants were used. This is of vital importance since it occurs at the top of the atmosphere (Zhang *et al.* 2012).

$$TB = \frac{k_2}{\ln\left[\left(\frac{k_1}{L\lambda}\right)+1\right]} - 273.15 \quad \textbf{(5)}$$

where TB is in ℃, k_1 is the band-specific thermal conversion constant (in watts/square meter × ster × μ) and k_2 in degrees Kelvin, $L\lambda$ is the spectral radiance. The constants $k_1$and k_2 were taken from the metadata of each satellite image.

Surface temperature (Ts)

The Earth's surface temperature was determined from surface brightness and emissivity temperature data. Three maps of land surface temperatures were created between the months of January, August and September. During the three months, the presence of clouds in different proportions was evident, altering their defining values. For its calculation, Equation 6 described by Avdan & Jovanovska (2016) for the sensor brightness and emissivity values were used.

$$Ts = \frac{TB}{\left\{1 + \left[\left(\frac{\lambda * TB}{\rho}\right) * \ln \varepsilon\lambda\right]\right\}} \quad \textbf{(6)}$$

where Ts is in ℃, λ is the wavelength of the emitted radiation (for which the maximum response and the average of the limiting wavelength were used (= 10.895), ρ is a constant determined by Equation 7.

$$\rho = h * \frac{c}{\sigma} = 1.438 * 10^{-2} mK \quad \textbf{(7)}$$

where σ is Boltzmann's constant (1.38 × 10−23 J/K), h is Planck's constant (6.626 × 10−34 J s), and c is the speed of light (2.998 × 108 m/s).

Estimated methane emission

The empirical model was a determination of the surface temperature to establish the temperature factor using the satellite thermal zone formula was expressed in Equation 8.

$$F_t = \frac{e^{0{,}334\,(\mathrm{Ts}-23)}}{1} + e^{0{,}334(\mathrm{Ts}-23)} \quad \textbf{(8)}$$

where e is the Euler value. The methane estimation model used is presented in Equation 9. Experiments have shown that the optimal temperature for most methanogens ranges between 30 °C and 40 °C. The flow value is extracted from the EDGAR database of Ecuador (EDGAR 2020), being an estimate determined to understand the levels of methane emitted by various countries in the world.

$$E_{CH4} = E_t * F_t \quad \textbf{(9)}$$

where E_{CH4} is the estimated CH_4 emission, E_t is the observed CH_4 flux and F_t is the temperature factor (dimensionless).

Table 1. Average CH4 emission from the Emissions Database for Global Atmospheric Research (EDGAR) in Megatonnes (Mt) of Ecuador.

Year	Observed CH_4 flux	Reference
2013	0.83	
2016	0.88	EDGAR (2020)
2020	0.97	

Analysis of data

In this research, all data processing was carried out in ArcGIS 10.8 software. The coordinate system and basic spatial processing were established. The spatial distribution of CH_4 emissions was presented using the surface temperature-based model in ArcGIS 10.8 with the Raster Calculator tool. Statistical analyzes of CH_4 emission were performed using zone statistics, thus determining maximum, minimum, average and standard deviation values. In addition to the rate of annual issue for the different periods. The spatial data obtained were processed in Excel 2019, through frequency statistics techniques.

RESULTS

Correlation analysis of surface temperature and NDVI

The NDVI values reached minimum values of up to -0.003, this is because there are areas with clouds or bodies of water, as it is a populated area (community). There are mostly areas without vegetation cover and therefore the NDVI values predominate between -0.003 and 0.6. The maximum NDVI values reach up to 0.6 and in a few places up to 0.7, such as protected forest areas. Mostly in community settlements, low NDVI values are observed. The spatio-temporal reduction of vegetation areas is also observed, mainly in September. Fig. 4 shows the NDVI maps that were obtained from the three satellite images worked on.

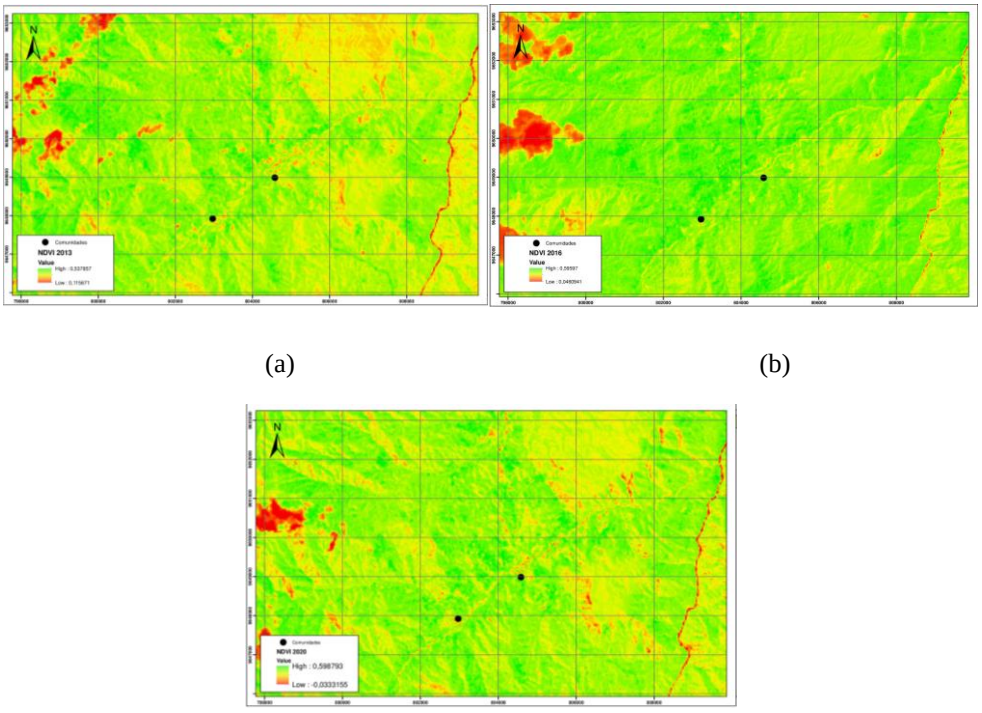

(a) (b)

(c)

Fig. 4. Spatial distribution of NDVI; (a) September 2, 2013; (b) January 14, 2016; and (c) August 4, 2020.

As a result of the analysis of the maps, the statistical values of the NDVI for 2013, 2016 and 2020 were determined (Table 2). It was found that the minimum NDVI value was -0.033 corresponding to the rivers within the communities and cloud cover; with a maximum value of 0.6 belonging to native forest areas.

Table 2. Statistical values of the NDVI of the study area for 2013, 2016 and 2020. V_{min}: Minimum values, V_{max}: Maximum values, μ NDVI: average NDVI, and σ: Standard deviation.

Year	V_{min}	V_{max}	μ NDVI	σ
2013	0.116	0.537	0.419	4,657
2016	0.046	0.596	0.431	8,240
2020	-0.003	0.599	0.427	6,159

The results of the surface temperature with higher values are seen in August 2020, most of them present similar trends according to their intensity distribution in certain sectors. Fig. 5 shows that in the part where the communities are located, the temperature is higher in bare soils and lower values in vegetative areas. Table 3 depicts the results of the analysis of the three maps. Minimum temperature values of 5.9 °C and maximum values of 26 °C were determined, with an annual average of 17.5, 21.7 and 22.9, for 2013, 2016 and 2020, respectively. Within the correlation between NDVI and surface temperature, an inverse trend was obtained to the spatial set as illustrated in Figs. 4 and 5. The NDVI values in grasslands were higher, while the temperature in communal spaces and bare areas were much higher than grasses. Given that water is a special case, here, the values are lower, since

the influence of surface-based vegetation comes from underlying areas that store transpiration due to evaporation and heat exchange. This caloric capacity that lacks vegetative cover, remains dry from not evapotranspirating, thus altering the variables under study.

Table 3. Statistical values of the surface temperature in ℃ in the study area for 2013, 2016 and 2020. V_{min}: Minimum values, V_{max}: Maximum values, μ T: Average temperature, and σ: Standard deviation.

Year	V_{min}	V_{max}	μT	σ
2013	5.9	18	17.5	1.29
2016	9.7	24	21.7	2.07
2020	8.1	26	22.9	1.43

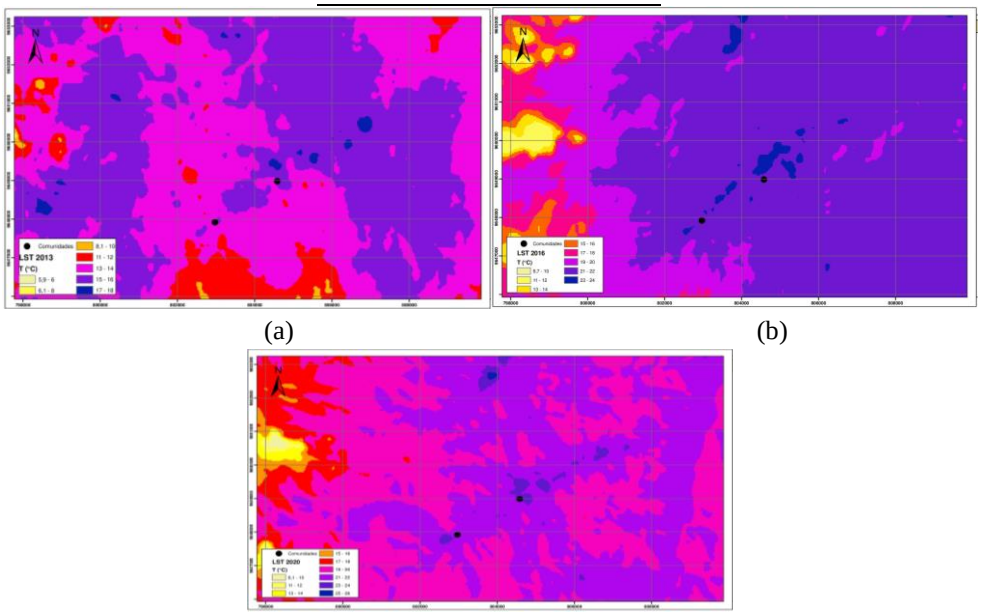

(a) (b)

(c)

Fig. 5. Spatial distribution of surface temperature; (a) September 2, 2013; (b) January 14, 2016; and (c) August 4, 2020.

CH_4 emissions

The statistical values determined the average methane emissions to be 1.18×10^{-4} Megatons (Mt) for 2013, 2016 and 2020. The year exhibiting higher values was 2020 with 2.36×10^{-4} Mt, while the lowest was 2013, with 1.74×10^{-5} Mt. There were significant differences in CH_4 emissions between the grids (Fig. 6). The highest emissions (>2.67×10^{-4} Mt) were recorded in communes and bare soils, while the lowest within forested areas and pastures, thus presenting regional differences.

Table 4. Statistical values of CH_4 emissions in Megatons/year in the study area for 2013, 2016 and 2020; V_{min}: Minimum values, V_{max}: Maximum values, μT: Average temperature, and σ: Standard deviation.

Year	V_{min}	V_{max}	μT	σ
2013	1.30×10^{-6}	5.36×10^{-5}	1.74×10^{-5}	6.29×10^{-6}
2016	2.11×10^{-4}	4.29×10^{-6}	1.01×10^{-4}	3.48×10^{-5}
2020	2.76×10^{-6}	2.67×10^{-4}	2.36×10^{-4}	2.86×10^{-5}

DISCUSSION

According to the results of the surface temperature, the values agree with El-Hattab *et al.* (2018) , where it was mentioned that rural areas present higher temperature data. This may occur due to bare soils and the type of soil. NDVI values are inversely related to temperature as stated by Zhang *et al.* (2012), which may be due to the amount of vegetation in the area that regulates the temperature. Likewise, based on the results of the water masses (Coelho & Correa 2013), they have a notable influence on the conditioning variables, having a direct effect on the

ambient temperature. So that, by elevating the ecological level within the communes, the tropical effect will increase. The methane estimation was carried out by testing the empirical model based on the surface temperature of the land and vegetation, which until a few years ago was applied to wetlands. During the summer, emissions will decrease due to precipitation and lower temperatures (Agarwal & Garg 2009), being applied in Tungurahua, Ecuador to estimate the amount of CH_4 emissions in a Landfill (Ambuludi *et al.* 2022). The model was applied for the first time in Mexico by Cortez (2015), in agreement with the fact that the method is reliable and can be adjusted according to the climatic conditions of each area.

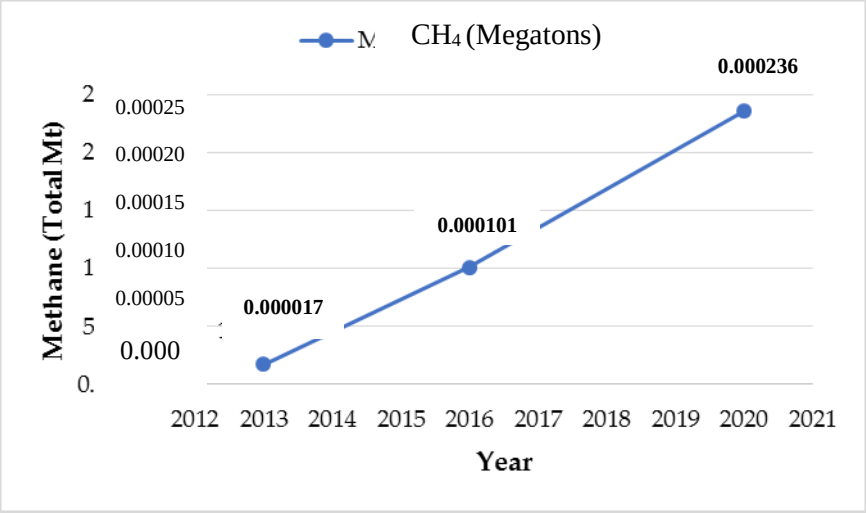

Fig. 6. Estimation of CH_4 emissions by the USEPA Mexican Model for 2013, 2016 and 2020.

A drawback with this type of model is the quality of the images that are available, since the more clouds there are, the less veracity of the results there is. This includes the lower monthly availability of cloud-free satellite images, necessary to acquire information (Ayasse *et al.* 2019).

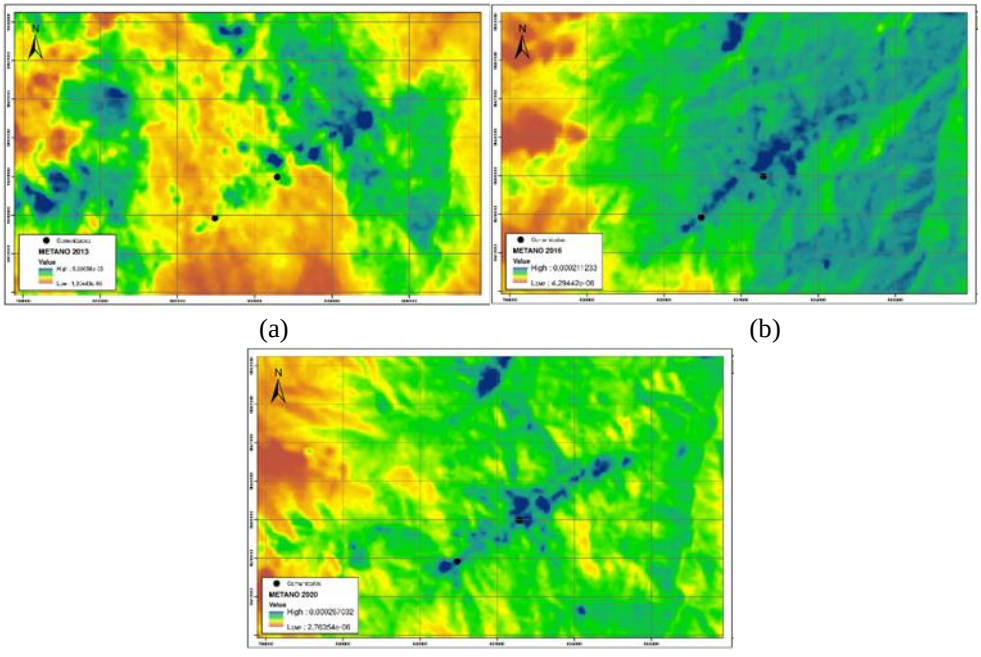

Fig. 7. Spatial distribution of the methane estimation of the Warints and Yawi communities; (a) September 2, 2013; (b) January 14, 2016; and (c) August 4, 2020.

Methane emissions increase in winter (Zhang *et al.* 2012) , due to intense rainfall, thus elevating the surface area of humid areas. The value of the annual emission growth rate for the period 2013-2020 experienced a value greater than 45% according to Sun *et al.* (2017). This is due to population growth and consequently deforestation that has caused the stripping of the native cover of the area.

CONCLUSION

The estimated methane (CH_4) emissions for the communities of Warints and Yawi were obtained through satellite images, for the years 2013, 2016 and 2020. It was 1.74×10^{-5}, 1.01×10^{-4} and 2.36×10^{-4} megatons, respectively, for an area of 107.62 km^2. In the period 2013-2020, an annual emission rate of 45.11% was obtained. The study found a high variability of methane emissions in the communes and bare soils, while the lowest were recorded within forested and pasture areas, presenting regional differences. Surface temperature and NDVI were the main factors within methane emissions, presenting average values of up to 26° C and 0.6, respectively, being uncertainties due to changes in flow and climatic conditions. This model is suitable for estimating the annual methane budget in areas with high vegetative incidence at both the local and regional levels.

REFERENCES

Agarwal, R & Garg, JK 2009, Methane emission modelling from wetlands and waterlogged areas using MODIS data. *Current Science*, 96: 36-40.

Akumu, CE, Pathirana, S, Baban, S & Bucher, D 2010, Modelling methane emission from wetlands in North-Eastern New South Wales, Australia using Landsat ETM+. *Remote Sensing*, 2: 1378-99.

Ambuludi, R, Carvajal, V & Diéguez, K 2022, Estimation of methane gas using the LandGEM model of the Patate-Pelileo municipal solid waste landfill, Tungurahua, Ecuador. *Technology in March Magazine*, 35: 67-78.

Arteaga, M 2017, Estimation of the capture level for greenhouse gases (carbon dioxide, nitrous oxide and methane) for the active reforestation project, in the forest reserve area of the Las Ceibas River basin, municipality of Neiva. De La Salle University, Faculty of Engineering. Environmental and Sanitary Engineering.

Avdan, U & Jovanovska, G 2016, Algorithm for automated mapping of land surface temperature using LANDSAT 8 satellite data. *Journal of Sensors*, 1:e1480307.

Ayasse, AK, Dennison, PE, Foote, M, Thorpe, AK, Joshi, S, Green, RO, Duren, RM, Thompson, DR & Roberts, DA 2019, Methane mapping with future satellite imaging spectrometers. *Remote Sensing*, 11: 3054.

Bautista, R, Constante, P, Gordon, A & Mendoza, D 2019, Design and implementation of an artificial vision system for analysis of NDVI data in spectral images of broccoli crops obtained using a remotely piloted aircraft. *Infoscience*, 12: 30.

Burkhanov, AU, Yadgarov, AA, Saidova, ME & Tugizova, MS 2024, Agricultural insurance protection and food security in the face of global climate change. Development of International Entrepreneurship Based on Corporate Accounting and Reporting According to IFRS*: Part B*, pp. 75-79.

Coelho, A & Correa, W 2013, Celsius surface temperature of the TIRS/Landsat-8 sensor: Methodology and applications. *Academic Geographical Journal*, 7: 31.

Cortez, A 2015, Estimation of methane emissions from the Bordo Poniente Landfill using satellite images.

EDGAR 2020, Ecuador - Methane emissions.

El-Hattab, M, Amany, SM & Lamia, GE 2018, Monitoring and assessment of urban heat islands over the southern region of Cairo Governorate, Egypt. *The Egyptian Journal of Remote Sensing and Space Science*, 21: 311-323.

Hantson, S, Chuvieco Salinero, E, Pons, X, Domingo Marimón, C, Cea, C & Moré, G 2011, Standard pre-processing chain for Landsat images of the National Remote Sensing Plan. *Remote Sensing Magazine: Magazine of the Spanish Remote Sensing Association*, 36: 51-61.

Janampa, S & Ponce, JJ 2022, Multi-temporal analysis of deforestation by satellite images in the district of Pangoa, Junín from 2000 to 2020. Universidad Continental.

PDOT 2015, Territorial development and planning plan of the Limón Indanza Canton.

Puliafito, SE, Bolaño-Ortiz, T, Berná, L & Pascual Flores, R 2020, High resolution inventory of atmospheric emissions from livestock production, agriculture, and biomass burning sectors of Argentina. *Atmospheric Environment*, 223: 117248.

Sanucci, C 2021, Evaluation of methane levels in oil production areas through the use of satellite images under the data science approach. National University of La Plata.

Stathopoulou, M, Cartalis, C & Petrakis, M 2007, Integrating Corine Land Cover data and Landsat TM for surface emissivity definition: application to the urban area of Athens, Greece. *International Journal of Remote Sensing*, 28: 3291-304.

Suárez, E & Acosta, K 2020, Multitemporal analysis of the vegetation cover of the municipality of Samacá, generated by socioeconomic activities.

Sucapuca Mamani, RO 2019, Urban heat islands through satellite images in the city of Juliaca during the year 2019. National University of Juliaca.

Sun, M, Zhang, Y, Ma, J, Yuan, W, Li, X & Cheng, X 2017, Satellite data based estimation of methane emissions from rice paddies in the Sanjiang Plain in northeast China. *PLOS ONE*, 12: e0176765.

Zhang, Y, Yiyun, C, Qing, D & Jiang, P 2012, Study on Urban Heat Island Effect Based on Normalized Difference Vegetated Index: A Case Study of Wuhan City. *Procedia Environmental Sciences*, 13: 574-81.

Bibliographic information of this paper for citing:

López, S, Haro, J, Haro, C, Carrillo, W, Narvaez Brito, JM, Usmanovich, BA, Tulakov, U, Erkinjon, T, Baxtiyarjon, M, Xalilillayevich, MZ 2025, Spatial evaluation of methane emissions in the communities of Warints and Yawi, Ecuador, Caspian Journal of Environmental Sciences, 23: 71-80.